**e-ISSN:** 2564-7954 CUSJE 21(01): 054-062 (2024) Research Article

Çankaya University

**Journal of Science and Engineering**

https://dergipark.org.tr/cankujse

CUJSE

# Investigation of Apatite Formation in MAX and MXene Alloy Foams

Merve ÖZKAN[1*]

[1] Department of Materials Science and Engineering, Çankaya University, Ankara

**Keywords**

MAX Alloy,
MXene Alloy,
Foams,
Apatite.

**Abstract**

In this study, synthesis of $Ti_3AlC_2$ MAX and $Ti_3C_2T_x$ MXene alloy powders was carried out, followed by the production and characterization of porous structures of $Ti_3AlC_2$ MAX and $Ti_3C_2T_x$ MXene alloys for biomedical applications, for instance, MAX and MXene alloys can be utilized as composites for implants or grafts. MAX alloy foams were produced using the space holder method to investigate apatite formation using simulated body fluid. Subsequently, MXene alloy foams were synthesized via chemical etching using the produced MAX alloy foams. MAX and MXene foams, after being immersed in simulated body fluid for 1, 5, 15, and 25 days, were characterized using SEM, XRD, and EDS techniques to examine the formation of apatite.

## 1. Introduction

Since the discovery of single-layer graphene synthesized from graphite in 2000, two-dimensional (2D) materials have emerged as popular alternatives to graphene in various application domains [1]. The discovery of new 2D materials has become necessary due to the potential for increasing quality of life through the usage of 2D materials in a variety of technical domains [1-3]. MXene alloys, which have been included in the field of two-dimensional materials since 2011 [4], have recently gained a lot of interest by researchers since they provide different features.

2D MXene alloys, composed of transition metals, carbon, and nitrogen, marked the beginning in a new age in nanotechnology [5]. In addition to having a layered structure with customizable surface terminations, they have good electrical, thermal, and optical qualities [6-9]. The use of MXene alloys as composites has also made it possible to assemble conventional devices and achieve more effective results in biomedical [10,11], energy [12], and sensor applications [13], owing to their large surface areas and customizable surface terminations [9-13]. Due to these properties, MXene alloys are still being investigated for a wide range of applications in biomedical (such as bioimaging, biosensing, antibacterial, DNA-related) [10,11] , energy (including energy storage, batteries) [12], sensor technology [13], catalysis, optics (such as Surface-enhanced Raman scattering (SERS), CO2 reduction), electromagnetic (including antenna, electromagnetic interference (EMI)) fields [9]. MXene alloys are typically synthesized using the chemical etching method with 3D MAX alloys as precusor materials [4]. The general chemical formula of MAX alloys is represented as $M_{n+1}AX_n$, where 'M' denotes early transition metals, 'A' denotes group A elements, and X represents either nitrogen or carbon. One of the most important features of this structure is the weak bonds between M and A, while the bonds between M and X are strong. Based on this characteristic, MXene alloys with the general formula $M_{n+1}X_nT_x$ are obtained by breaking the weak bonds through chemical etching and removing the A element and $T_x$ denotes surface terminations such as -O, -F, -OH [4,9]. Thus, it can be understood that the choice of raw material and synthesis processes are crucial for efficiently achieving the desired structure and adjusting surface terminations as desired in MXene alloys. The chemical etching method is also an excellent technique for altering the properties of MXene alloys [14], and the schematic representation of this method is provided in Figure 1b. Depending on the characteristics of the etching

*Corresponding Author: merveozkan758@gmail.com
Received: March 19, 2024, Accepted: April 27, 2024

solution used during the process, surface terminations can be modified, and shapes, sizes, and layer numbers can be adjusted accordingly. The ability to tailor the process according to desired properties makes MXene alloys an excellent choice for various application areas.

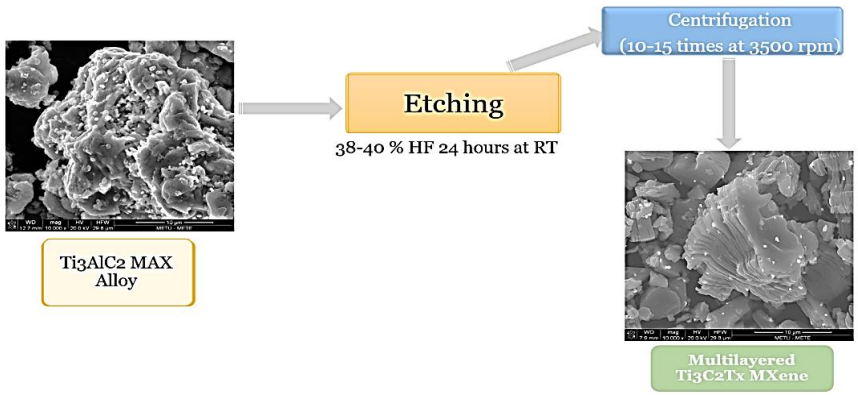


**Figure 1.** Schematic representation of selective etching method.

MXene alloys are typically synthesized using the chemical etching method with 3D MAX alloys as precusor materials [4]. The general chemical formula of MAX alloys is represented as $M_{n+1}AX_n$, where 'M' denotes early transition metals, 'A' denotes group A elements, and X represents either nitrogen or carbon. One of the most important features of this structure is the weak bonds between M and A, while the bonds between M and X are strong. Based on this characteristic, MXene alloys with the general formula $M_{n+1}X_nT_x$ are obtained by breaking the weak bonds through chemical etching and removing the A element and $T_x$ denotes surface terminations such as -O, -F, -OH [4,9]. Thus, it can be understood that the choice of raw material and synthesis processes are crucial for efficiently achieving the desired structure and adjusting surface terminations as desired in MXene alloys. The chemical etching method is also an excellent technique for altering the properties of MXene alloys [14], and the schematic representation of this method is provided in Figure 1b. Depending on the characteristics of the etching solution used during the process, surface terminations can be modified, and shapes, sizes, and layer numbers can be adjusted accordingly. The ability to tailor the process according to desired properties makes MXene alloys an excellent choice for various application areas.

Since its first synthesis in 2011 using hydrofluoric acid (HF) from the $Ti_3AlC_2$ MAX alloy, the $Ti_3C_2T_x$ MXene alloy has been the subject of extensive research and studies and the electron microscope images of $Ti_3AlC_2$ MAX alloy and $Ti_3C_2T_x$ MXene alloy are presented in Figure 2, respectively [4]. MXene alloys are being investigated for various applications in the biomedical field, including imaging technologies, drug delivery systems, biosensors, antibacterial application, and wearable devices, among others [14-16].

When examining the conducted studies, promising results have been obtained. However, there has been no study specifically investigating the biocompatibility of porous MXene alloys synthesized from porous MAX alloys using HF. In this study, simulated body fluid experiments were conducted to successfully test the biocompatibility property and address this gap.

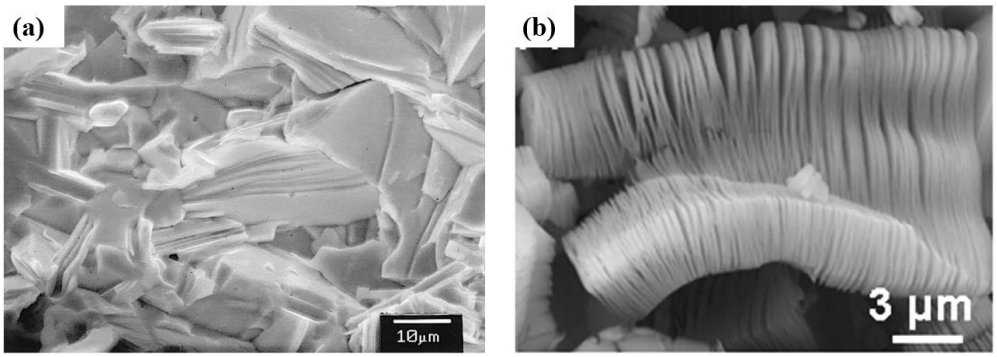


**Figure 2.** SEM images of (a) $Ti_3AlC_2$ MAX alloy and (b) $Ti_3C_2T_x$ MXene alloy. Reprinted from [17] and [14].

## 2. Experimental Study

### 2.1. Production of $Ti_3AlC_2$ MAX Foams

To produce porous $Ti_3AlC_2$ MAX alloy, $Ti_3AlC_2$ MAX powder obtained from Alfa Aesar was mixed with urea powder particles ranging in size from 300 to 500 micrometers. Cold pressing at 500 MPa pressure was then applied to the mixture. Subsequently, the green body was immersed in deionized water at room temperature for 24 hours to remove the urea particles. The green body was then dried in a vacuum oven at 60 °C and subjected to a sintering process at 1400°C in a high purity argon atmosphere for 1 hour.

### 2.2. Synthesis of $Ti_3C_2T_x$ MXene Powder and Foams

To begin, 50 mL Eppendorf tubes, a bullet stirrer, and a 200 ml plastic sample cup were initially washed with 1 M HCl followed by rinsing with deionized water. Subsequently, 20 ml of HF (38-40%) was poured into the plastic sample cup, which was then placed on a hot plate with the mixing speed set to 300 rpm. Gradually, 1 gram of MAX powder was added in small increments over a period of 10 minutes. The MAX powder and acid solution were allowed to react for 24 hours, with the container tightly sealed to allow for the escape of gases produced during mixing.

After etching, 20 ml of the prepared mixture was evenly divided into two portions, with each 10 ml portion added to separate 50 ml Eppendorf tubes containing 40 ml of deionized water. Subsequently, these tubes were subjected to centrifugation (using an Elektro-mag M4800M centrifuge device) at 3500 rpm for 5 minutes. Upon completion of centrifugation, the pH of the solution was measured, following which the supernatant was decanted, and deionized water was added once again. This process was repeated several times until the pH value approached approximately 5.

Finally, the settled powders in the Eppendorf tubes were transferred to a glass container and dried under vacuum at 80 °C for a duration of 24 hours.

To synthesize MXene alloy foams, the produced MAX alloy foams were immersed in hydrofluoric acid at room temperature for 24 hours. Subsequently, they were washed with deionized water to remove HF residues, and this process was repeated until the pH reached approximately 5.

Subsequently, the produced foams were immersed in simulated body fluid (SBF) prepared according to the simulated body fluid recipe developed by Kokubo et al. [18]. They were specifically tested under controlled conditions at 36.5 °C ± 0.5 °C temperature and pH 7.4 for 1, 5, 15, and 25 days. During this process, to stabilize the ion concentration, the samples in SBF were refreshed every two days with a new SBF solution.

### 2.3. Characterization Techniques

The structures of the produced MAX and MXene foams were examined using "FEI 430 Nano Scanning Electron Microscopy" (SEM) equipped with an energy dispersive X-Ray spectroscopy (EDS) analyzer at 20 kV, and elemental analysis was conducted.

X-ray diffraction analysis was conducted to investigate the phases present in the samples produced. Structural analysis was performed using the "Bruker D8 Advance Eco model X-Ray Diffractometer" instrument. The $Ti_3AlC_2$ MAX alloy was scanned with Cu-Kα radiation over a continuous range of 10° to 80° 2θ angles at a scan speed of 1°/min. Conversely, $Ti_3C_2T_x$ MXene alloy powders were scanned over a range of 5° to 80° 2θ angles at a scan speed of 1°/min.

## 3. Results and Discussion

### 3.1. Production of MAX Foams

When macro and micro analysis was conducted on the produced MAX foams, pores resulting from the removal of carbamide particles were observed. The pore sizes were measured to be approximately 407 micrometers. Additionally, as seen in Figure 3c, micro-pores formed on the cell walls. The presence of macro and micro pores formed after partial sintering and their interconnected play a significant role in the transfer of body fluids within bone tissue.

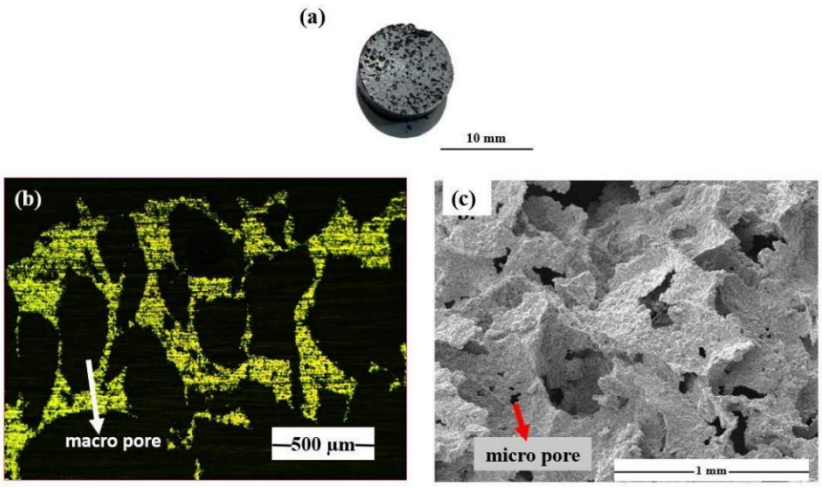


**Figure 3.** Respectively MAX alloy foam images (a) macro, (b) optical microscopy, and (c) SEM.

Furthermore, in Figure 4a, the image of the foamed MAX alloy is depicted. Figure 4b presents the EDS analysis conducted on this region. Upon examination of the EDS findings, the presence of Ti, Al, and C elements is observed as anticipated, alongside the presence of Si, likely originating from the initial powder. Additionally, Figure 5 displays the XRD analysis results, indicating a decrease in the TiC phase and an increase in the $Ti_3AlC_2$ phase.

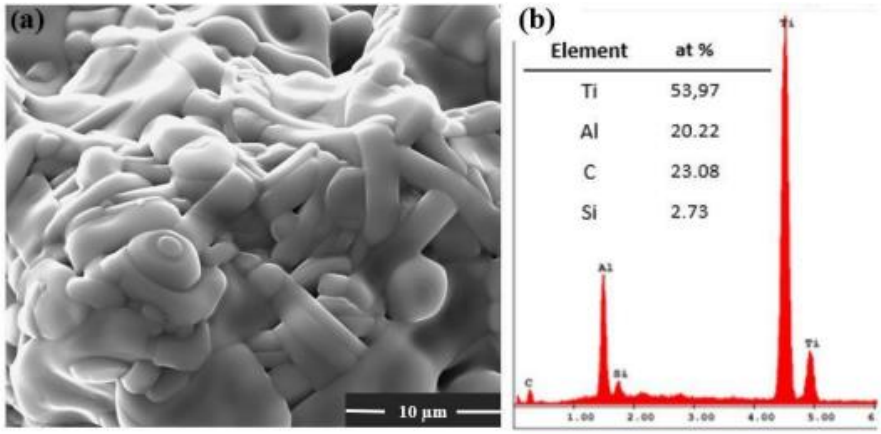


**Figure 4.** (a) SEM image of MAX alloy foam, (b) EDS analysis of MAX alloy foam.

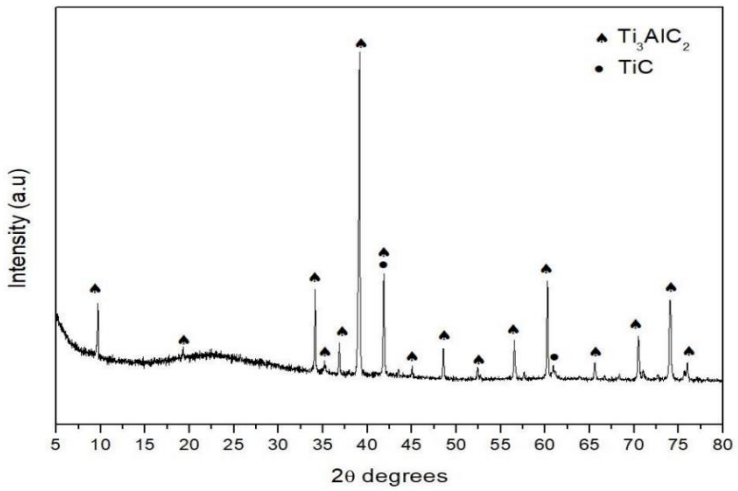


**Figure 5.** XRD analysis of MAX alloy foam.

### 3.2. Synthesis of MXene Alloy Foams

As previously described in the methods section, MXene foam alloys synthesized from MAX foams were examined, revealing similar pore sizes and the presence of micro and macro pores, as depicted in Figure 6. Additionally, unlike previous studies where powder MAX was utilized to produce MXene alloys, here, porous MAX alloy served as the initial sample. Upon examination of SEM images in Figures 7a and 7b, partially layered multilayered MXene regions can be observed. However, upon analysis of EDS results, a high percentage of Al element, approximately 4.75, was detected. These findings suggest a possibility that due to additional sintering of MAX foam, the surface area decreased, and HF may not have sufficiently penetrated. Nevertheless, examination of EDS results reveals similar proportions of F element between powder MXene and MXene foam, indicating that the etching process, although not completely effective, was highly successful. In Figure 8, SEM and EDS results of the powder MXene alloys synthesized from powder MAX alloys are provided.

**Figure 6.** (a) Macro image of MXene alloy foam, (b) Optical image taken from the crossection of MXene alloy foam and, (c) SEM image of MXene alloy foam.

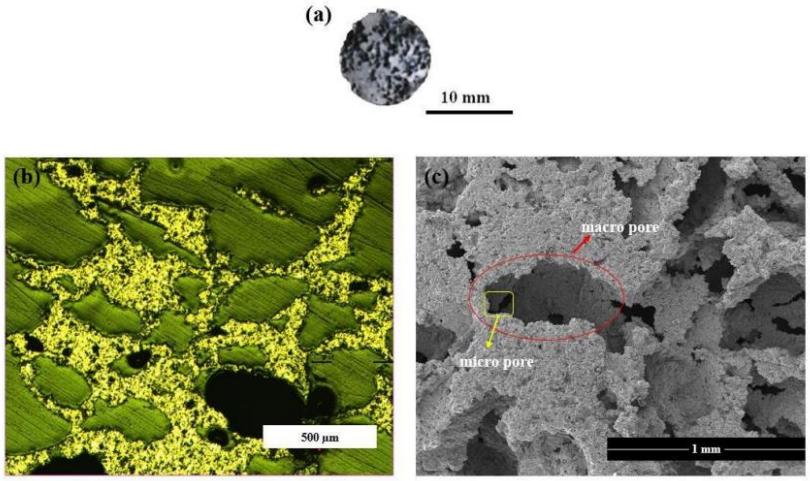


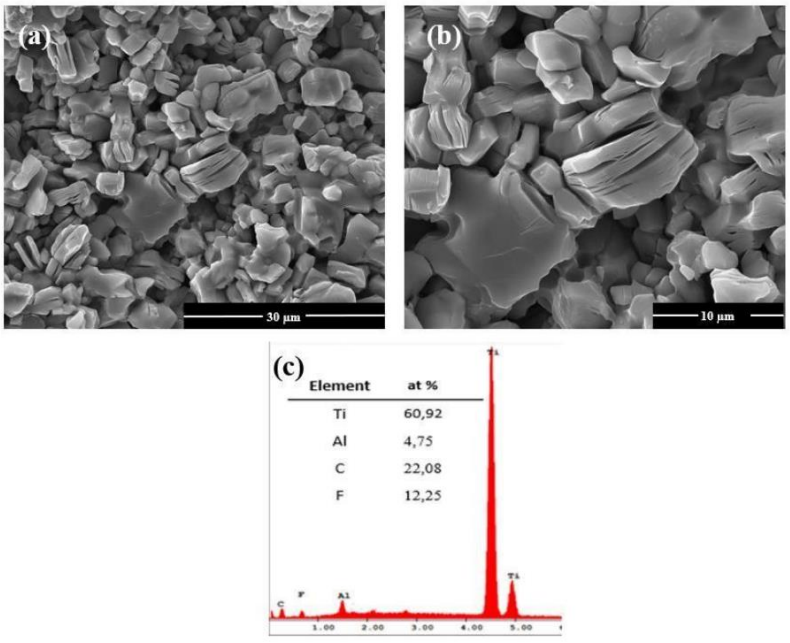


**Figure 7.** SEM images and EDS result of MXene alloy foam.

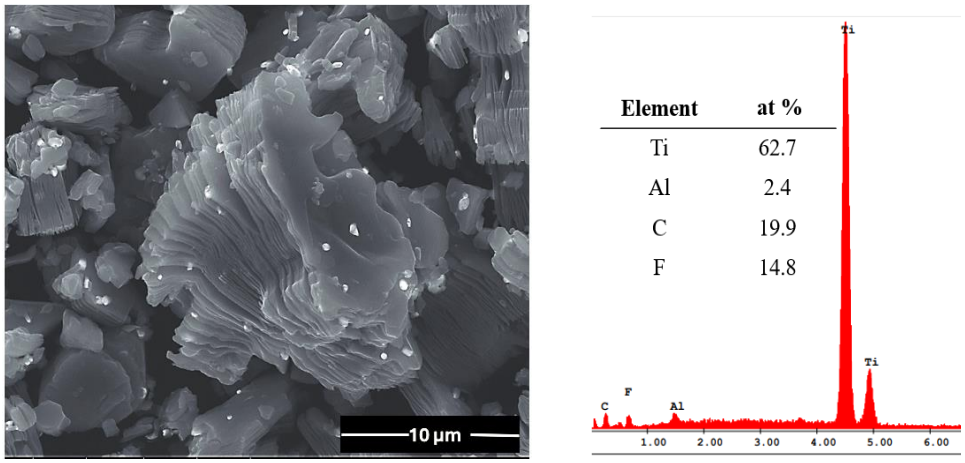


**Figure 8.** SEM image and EDS analysis of $Ti_3C_2T_x$ MXene powder.

## 4. Simulated Body Fluid Tests

The produced MAX and MXene alloy foams were immersed in SBF at 36.5 °C ± 0.5 °C for durations of 1, 5, 15, and 25 days to investigate relative apatite formation. Upon examination of the XRD results presented in Figure 9 for MAX and MXene alloys immersed in SBF at various time intervals, no apatite peaks were observed. However, analysis of the SEM images provided in Figure 10 revealed spherical apatite-like structures covering most of the cell walls of the MAX foam sample immersed in SBF for 15 days. Additionally, small white precipitates were observed in the MXene alloy foam sample after 1 day, but these precipitates did not grow even after 25 days. These results suggest that the precipitated phases in both MAX and MXene foam samples were not detected by XRD, possibly due to their coverage of the internal regions of the foams.

When examining the XRD graph provided in Figure 9, peaks in the range of 30 degrees are observed in MXene samples immersed in SBF for 5 and 25 days, as well as in MAX samples immersed in SBF for 15 and 25 days. The samples were provided in powder form for XRD analysis, and during the manual crushing process to powderize the samples, uniform force application could not be ensured for all samples. Therefore, the peaks observed differently from other samples are attributed to the deformation occurring during the sample preparation stage for characterization. Moreover, the other reason may be due to low amount of sample characterized by XRD. Signals may come from glass substrate during XRD characterization.

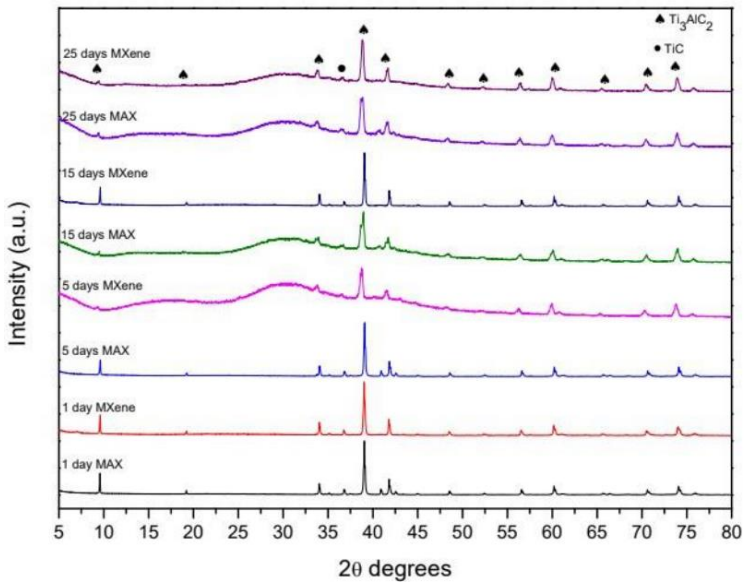


**Figure 9.** XRD results of MAX and MXene alloy foams immersed in SBF.

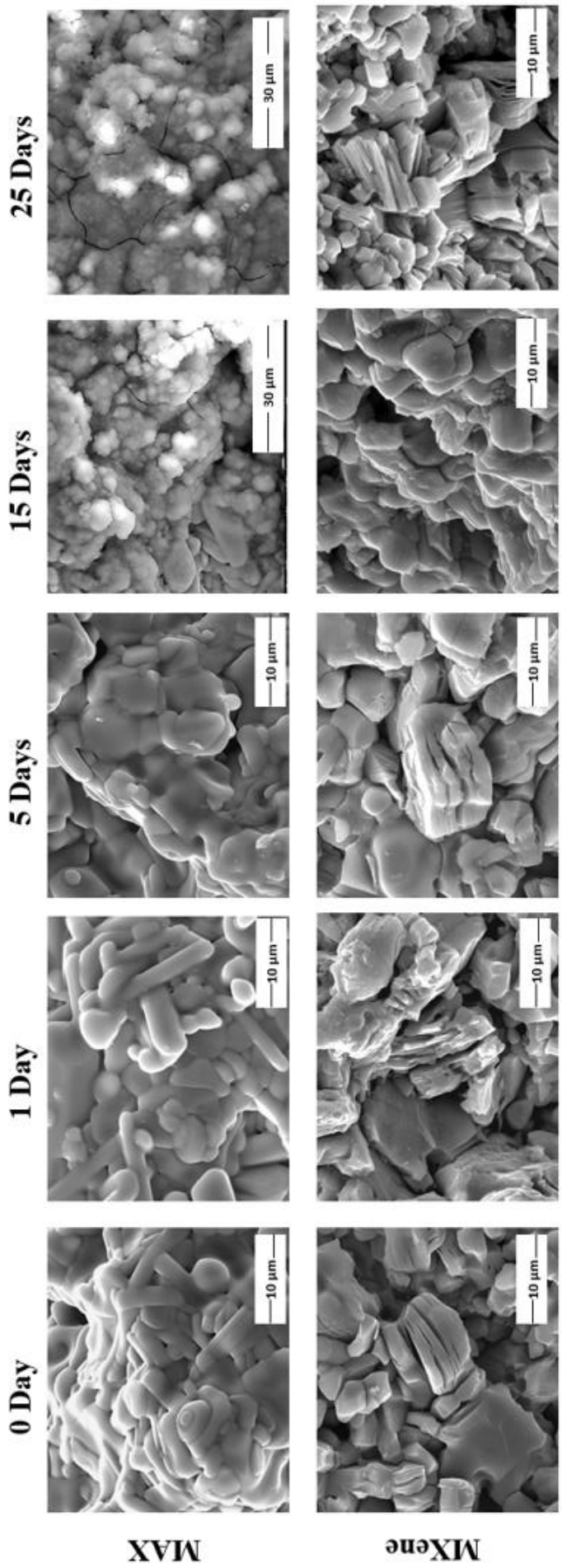


**Figure 10.** SEM images of MAX and MXene alloy foam samples soaked in SBF for 0, 1, 5, 15 and, 25 days.

The other purpose of incubating the samples in SBF is to investigate the atomic ratios of Ca and P elements, comparing the similarity of the atomic ratios of Ca/P elements in bone and synthetic hydroxyapatite. The Ca/P atomic ratios in bone and synthetic hydroxyapatite are 1.655 and 1.667, respectively. The Ca/P ratio obtained from EDS analysis of samples incubated in SBF is provided in Table 1. Upon examining these results, it is observed that in MXene alloys, only the Ca element precipitates in the first 5 days. After 15 days, the P element also precipitates, but the Ca/P ratio is 2.4, which is considerably high for the apatite form. However, after 25 days, the Ca/P ratio in MXene alloy foams approaches 1.8, similar to the ratio found in apatite. In MAX alloy foams, although apatite ratios are not observed in the first 5 days, after 15 days, the Ca/P ratio is 1.5, which is very close to the ratio found in apatite, confirming that the precipitated phase is apatite, and after 25 days, it is determined to have a ratio of 1.6, indicating that the precipitated phase is apatite. From these results, it is observed that MAX alloy foams have better apatite formation performance compared to MXene alloy foams. Due to the surface terminations of the MXene foam alloys synthesized with HF etching being fluorine-based, much less Ca and P precipitation occurs.

**Table 1.** Ca/P atomic ratio of MAX and MXene alloy foam samples immersed in SBF 1, 5, 15 and, 25 days.

| Element | at. % | | | | | | | |
|---|---|---|---|---|---|---|---|---|
| | 1 day immersion | | 5 days immersion | | 15 days immersion | | 25 days immersion | |
| | MAX | MXene | MAX | MXene | MAX | MXene | MAX | MXene |
| Ca | - | 1.0 | - | 1.4 | 26.9 | 2.0 | 36.6 | 2.2 |
| P | - | - | - | - | 18.4 | 0.80 | 23.2 | 1.2 |
| Ca/P | - | - | - | - | 1.5 | 2.4 | 1.6 | 1.8 |

## 5. Conclusions

In this study, $Ti_3C_2T_x$ MXene foam alloys were successfully synthesized via chemical etching from $Ti_3AlC_2$ MAX alloy foams initially obtained through partial sintering using the space holder method, despite not having been utilized as precursors for bulk samples previously. Subsequently, MAX and MXene alloy foams incubated in SBF at a constant temperature (36.5 °C ± 0.5) for various durations were analyzed for the atomic ratios of Ca and P elements to investigate the formation of apatite structures. It was observed that after 15 days, apatite formation in MAX alloy foams occurred at a level comparable to that of bone, while in MXene alloy foams, sufficient apatite formation was not observed due to the presence of Floren-based surface terminations derived from HF acid. From this study, it is understood that Floren-based surface terminations influence bioactivity. This study has provided guidance by utilizing floren-free etchants or alternative methods for etching processes to observe apatite formation in MXene alloys. In future studies, the investigation of the mechanical properties of MAX and MXene foam alloys opens promising avenues for research into their utilization as implants or grafts in biomedical applications.

## Acknowledgements

Author expresses her gratitude and deep thanks to her supervisors for their endless motivation, support, wisdom, and unique experiences guiding her. Author grateful to Assoc. Prof. Dr. Göknur Büke for her support.

## Declaration of Competing Interest

No conflict of interest was declared by the authors.

## Authorship Contribution Statement

**Merve ÖZKAN**: Writing, Reviewing, Editing, Analysis; Interpretation of Results and Manuscript Preparation.

## References


[1] A. K. Geim and K. S. Novoselov "The Rise of Graphene" *Nat. Mater.*, vol. 6, no. 3, pp. 183, 2007.

[2] V. Singh, D. Joung, L. Zhai, S. Das, S. I. Khondaker, and S. Seal, "Graphene based materials: Past, present and future," *Prog.Mater.Sci.*, vol. 56, no. 8, pp. 1178, 2011.

[3] Q. Tang, Z. Zhou, and Z. Chen, "Graphene-related nanomaterials: Tuning properties by functionalization," *Nanoscale*, vol. 5, no. 11, pp. 4541, 2013.

[4] M. Naguib, M. Kurtoglu, V. Presser, J. Lu, J. Niu, M. Heon, and M. W. Barsoum, "Two-dimensional nanocrystals produced by exfoliation of $Ti_3AlC_2$. " *Advanced Materials*, vol. 23, no. 37, pp. 4248–4253, 2011.

[5] Y. Gogotsi, and B. Anasori, "The Rise of MXenes." *ACS Nano*, vol. 13, pp. 8491–8494, 2019.

[6] A. Vahid Mohammadi, J. Rosen, and Y. Gogotsi, "The world of two-dimensional carbides and nitrides (MXenes)" *Science*, vol. 372, pp. eabf1581, 2021.

[7] Y. Gogotsi, and Q. Huang, "MXenes: Two-Dimensional Building Blocks for Future Materials and Devices." *ACS Nano*, vol. 15, pp. 5775–5780, 2021.

[8] A. Shayesteh Zeraati, et al. "Improved synthesis of $Ti_3C_2T_x$ MXenes resulting in exceptional electrical conductivity, high synthesis yield, and enhanced capacitance." *Nanoscale*, vol. 13, pp. 3572– 3580, 2021.

[9] B. Anasori, and Y. Gogotsi, "MXenes: trends, growth, and future directions." *Graphene and 2D Materials*, vol. 7, pp. 75–79, 2022.

[10] A. Maleki, M. Ghomi, N. Nikfarjam, M. Akbari, E. Sharifi, M. A. Shahbazi, and Y. Chen "Biomedical Applications of MXene-Integrated Composites: Regenerative Medicine, Infection Therapy, Cancer Treatment, and Biosensing", *Advanced Functional Materials*, vol. 32, no. 34, pp. 2203430, 2022.

[11] Y. Fu, J. B. Zhang, H. Lin, and A. Mo "2D titanium carbide (MXene) nanosheets and 1D hydroxyapatite nanowires into free standing nanocomposite membrane: in vitro and in vivo evaluations for bone regeneration", *Materials Science and Engineering C*, vol. 118, pp. 111367, 2021.

[12] S. Venkateshalu, and A. N. Grace, "MXenes-A new class of 2D layered materials: Synthesis, properties, applications as supercapacitor electrode and beyond", *Applied Materials Today*, vol. 18, pp. 100509, 2020.

[13] B. Fu, J. Sun, C. Wang, C. Shang, L. Xu, J. Li, and H. Zhang "MXenes: Synthesis, Optical Properties, and Applications in Ultrafast Photonics", *Small*, vol. 17, no. 11, pp. 2006054, 2021.

[14] M. Naguib, V. N. Mochalin, M.W. Barsoum, and Y. Gogotsi "25th anniversary article: MXenes: A new family of two-dimensional materials." *Advanced Materials*, vol. 26, pp. 992–1005, 2014.

[15] J. C. Lei, X. Zhang, and Z. Zhou "Recent advances in MXene: Preparation, properties, and applications." *Frontiers of Physics*, vol. 10, pp. 276–286, 2015.

[16] H. Lin, Y. Chen, and J. Shi "Insights into 2D MXenes for Versatile Biomedical Applications: Current Advances and Challenges Ahead", *Advanced Science*, vol. 5, no. 10, pp. 1800518, 2018.

[17] N. V. Tzenov, and M.W. Barsoum, "ChemInform Abstract: Synthesis and Characterization of $Ti_3AlC_2$." *ChemInform*, vol. 31, 2000.

[18] T. Kokubo, and H. Takadama, "How useful is SBF in predicting in vivo bone bioactivity?" *Biomaterials*, vol. 27, pp. 2907–2915, 2006.